Isomerization of the Prenucleation Building Unit during Crystallization of $AlPO_4$-CJ2: An MQMAS, CP-MQMAS, and HETCOR NMR Study

Francis Taulelle,*,† Marek Pruski,‡ Jean Paul Amoureux,§ David Lang,‡ Alain Bailly,‡,§ Clarisse Huguenard,† Mohamed Haouas,† Corine Gérardin,† Thierry Loiseau,⊥ and Gérard Férey⊥

Contribution from the RMN et Chimie du Solide, UMR 7510 ULP-Bruker-CNRS, Université Louis Pasteur, 4 rue Blaise Pascal, 67070 Strasbourg Cedex, France, Ames Laboratory, 230 Spedding Hall, Iowa State University, Ames, Iowa 50011, Laboratoire de Dynamique et Structure des Matériaux Moléculaires, URA 801, Bat. P5, UFR de Physique, Université des Sciences et Technologies de Lille, 59655 Villeneuve d'Ascq Cedex, France, and Institut Lavoisier, IREM UMR 173, Université de Versailles-Saint Quentin, 45 Avenue des Etats-Unis, 78035 Versailles Cedex, France

Received April 22, 1999. Revised Manuscript Received July 29, 1999

Abstract: The structure of $AlPO_4$-CJ2 aluminophosphate has been reinvestigated by MAS, MQMAS (multiple quantum magic angle spinning), CP-MQMAS (cross polarization-MQMAS), and HETCOR (heteronuclear correlation) NMR spectroscopy. The CP-MQMAS method showed that the sample, when not allowed adequate time for crystallization, included a substantial concentration of amorphous species. The crystalline component was cleanly singled out by this technique. We discuss the relative populations and the distributions of F and OH groups within the structural building units (SBUs) and the distribution of various SBUs within the crystalline structure of $AlPO_4$-CJ2. For the latter case, a mixture of SBUs is demonstrated from the $^{19}F \rightarrow {}^{31}P$ HETCOR spectrum. Prenucleation building units (PNBUs) are the principal objects used for efficient crystal formation. They may undergo an isomerization to reach the proper configuration to integrate into the solid network. The isomerization implies formation of a bridge within the PNBU, probably at random with respect to OH or F. As integration in the network is taking place parallel to isomerization, the network forms as domains containing a mixture of the different types of SBUs.

Introduction

$AlPO_4$-CJ2 (CJ2 as a short form) was first synthesized by Yu et al.[1] On the basis of X-ray diffraction data, they proposed a structure that did not contain any fluoride, though they stated that fluorides were present in the framework. This ambiguity is due to the inability of the X-ray studies to discriminate between OH and F, which have equal electronic densities. As the first structure analysis of $AlPO_4$-CJ2 could not conclusively establish the presence of fluorides, a second single-crystal study was performed on the same phase.[2] This time, in addition to XRD, an NMR study was also undertaken for structure determination.[3] Two distinct fluoride environments were clearly shown to be present in the polycrystalline sample. An isotypic phase of this compound was also obtained, using gallium instead of aluminum. The ^{19}F NMR spectrum of $GaPO_4$-CJ2, however, shows only one type of fluorine environment.[2] The variation in fluorine content between $AlPO_4$-CJ2 and $GaPO_4$-CJ2 is probably related to the different ionic radii of Ga and Al, inducing differences in topological constraints. In $AlPO_4$-CJ2, fluoride and hydroxyl groups are described as sharing a pair of nonequivalent sites with fractional site occupancies.[2,3] Other analogues of CJ2 have also been studied that do not contain fluorine[4,5] or that have partial substitution of aluminum by cobalt.[6]

In a general study of solid formation of microporous aluminophosphates,[7,8] $AlPO_4$-CJ2 has been selected as a good model for characterizing the various stages of condensation from primary building units in solution to the crystalline solid phase. Its synthesis has been the object of a systematic multinuclear NMR analysis, in situ as well as ex situ, in which both the supernatant liquid and the solid phases obtained at various stages of synthesis have been analyzed.[8−10] These studies have shown that the synthesis occurs through a sequence of steps.[8−10] Formation of an amorphous oxyfluorinated phase occurs first,

* To whom correspondence should be addressed. E-mail: taulelle@chimie.u-strasbg.fr.

† Université Louis Pasteur.

‡ Iowa State University.

§ Université des Sciences et Technologies de Lille.

⊥ Université de Versailles-Saint Quentin.

(1) Yu, L.; Pang, W.; Li, L. *J. Solid State Chem.* **1990**, *87*, 241.

(2) Ferey, G.; Loiseau, T.; Lacorre, P.; Taulelle, F. *J. Solid State Chem.* **1993**, *105*, 179.

(3) Taulelle, F.; Loiseau, T.; Maquet, J.; Livage, J.; Ferey *J. Solid State Chem.* **1993**, *105*, 191.

(4) Dick, S.; Gossner, U.; Grossman, G.; Ohms, G.; Zeiske, T. *Z. Naturforsch.* **1997**, *52b*, 1439.

(5) Dick, S.; Grossman, G.; Ohms, G.; Müller, M. *Z. Naturforsch.* **1997**, *52b*, 1447.

(6) Logar, N. Z.; Golic, L.; Kaucic, V. *Microporous Mater.* **1997**, *9*, 63.

(7) Gerardin, C.; In, M.; Allouche, L.; Haouas, M.; Taulelle, F. *Chem. Mater.* **1999**, *11*, 1285.

(8) Haouas, M. In *Etude RMN de la synthèse hydrothermale des aluminophosphates micropreux oxyfluorés: AlPO4−CJ2, ULM-3 et ULM-4*; Haouas, M., Ed.; University Louis Pasteur: Strasbourg, France, 1999; p 259.

(9) Taulelle, F.; Haouas, M.; Gerardin, C.; Estournes, C.; Loiseau, T.; Ferey, G. *Colloids Surf. A* **1999**, *158*, 299.

(10) In-Gerardin, C.; In, M.; Taulelle, F. *J. Chim. Phys.* **1995**, *92*, 1877.

10.1021/ja991295n CCC: $18.00
Published on Web 12/08/1999

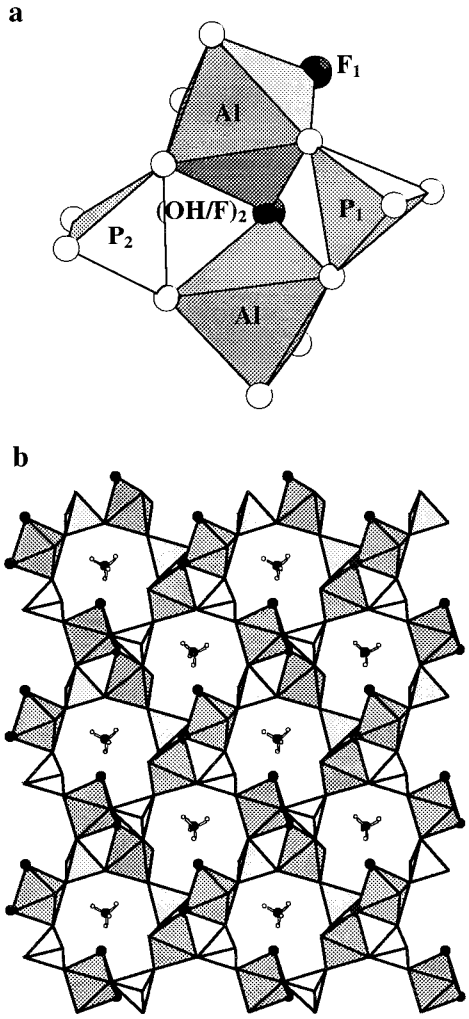

Figure 1. (a) Structural building unit (SBU) of $AlPO_4$-CJ2. (b) Polyhedral view of CJ2 crystal along the [100] direction.

followed by its phosphatation and dissolution into a fluorophosphato-aluminate species. An aluminum complex of general formula $AlF(H_2PO_4)(H_2O)_{3-x}(OH)_x$ forms in solution, in which aluminum exhibits 5-fold coordination. This complex can then further condense to give a prenucleation building unit,[11] which we believe is a dimer of the simple complex. This species only contains aluminum atoms that are 5-fold coordinated. Crystallization of CJ2 begins while several amorphous solids coexist.

No aluminum coordination state higher than 5 is observed in solution[8] while the crystals grow. However, our earlier XRD study showed that crystalline $AlPO_4$-CJ2 consists of structural building units (SBUs) that contain two crystallographically inequivalent sites for each aluminum and phosphorus atom, as depicted in Figure 1a.[2] In the SBU, phosphorus and aluminum atoms are alternating and form a square-like unit. One aluminum atom is 5-fold coordinated, while the other one is 6-fold coordinated. Both have four oxygen atoms in their coordination sphere that also connect them to the phosphorus atoms. Two of the oxygen atoms connect inside the structural unit, and two make external connections. The pentacoordinated aluminum shares a bridging group with the hexacoordinated aluminum, which has also a bond to a terminal site. OH or F can occupy the bridging and terminal sites with fractional occupancies that will be discussed later. Let us denote the atoms in bridging and terminal positions by X_b and X_t, respectively, regardless of their occupancies by OH or F.[2] Using this notation, the nearest-neighbor distances $d(P,X)$ are as follows: P_1-type phosphorus has one X_t neighbor and one X_b neighbor at distances $d(P_1,X_t) = 3.55$ Å and $d(P_1,X_b) = 3.06$ Å, while P_2-type phosphorus is surrounded by two X_t sites at $d(P_2,X_t) = 3.49$ and 3.56 Å, as well as two X_b sites at $d(P_2,X_b) = 2.91$ and 3.23 Å.

Solid-state NMR spectroscopy is our tool of choice to address several unsettled questions regarding the structure of $AlPO_4$-CJ2 crystals. The isotropic data for each of the ^{27}Al environments are resolved using MQMAS methods. Phase mixtures or impurities, if present, can be edited using CP-MQMAS of ^{27}Al with polarization transfer from ^1H or ^{19}F. Connectivity of the fluorine nuclei with aluminum or phosphorus nuclei is determined using $^{19}F-^{27}Al$ and $^{19}F-^{31}P$ HETCOR experiments. We are particularly interested in the relative occupancy of the bridged and terminal groups by fluorine and OH groups in the SBUs and in the distribution of various SBUs within the $AlPO_4$-CJ2 crystals.

Experimental Section

Synthesis of $AlPO_4$-CJ2. $AlPO_4$-CJ2 is a microporous aluminophosphate obtained by hydrothermal synthesis. The reaction mixtures having molecular ratio 1 Al_2O_3:1 P_2O_5:1 hexamethylenetetramine:2 NH_4F:80 H_2O were placed in a stainless steel autoclave lined with Teflon and heated at 180 °C for several days. The resulting products were filtered off, washed with distilled water, and then dried at room temperature. A polycrystalline sample could usually be obtained after several days of synthesis. Large single crystals (about 0.2 mm/side) can be obtained after a longer thermal treatment. More details about the synthesis process can be found in previous descriptions.[2,8]

Two different CJ2 samples were prepared for this study: (i) a "contaminated" sample referred to as CJ2(c) that was synthesized over a period of only 1 day, and is therefore likely to contain a significant concentration of undesired phases; and (ii) a sample that was hydrothermally treated for an additional week, which is expected to show a higher degree of structural purity and is henceforth referred to as CJ2(p).

The chemical formula for CJ2 can be written as $(N1H_4)_1(N2H_4)_{0.78}(H_3O)_{0.22}(Al1)_1(Al2)_1(P1O_4)_1(P2O_4)_1(F1)_x(OH1)_{1-x}(F2)_y(OH2)_{1-y}$. In the sample synthesized in our earlier study,[3] we used the chemical elemental analysis and MAS NMR to determine its chemical formula, $x = 1.0$ and $y = 0.33$. The reduced formula could be written as $(NH_4)_{0.89}(H_3O)_{0.11}(Al)_{1.0}(PO_4)_{1.0}(OH)_{0.33}(F)_{0.67}$. Using quantitative NMR measurements of ^{19}F, as described in the section below, a slightly different reduced formula was determined for the samples used in this study, $(NH_4)_{0.89}(H_3O)_{0.11}(Al)_{1.0}(PO_4)_{1.0}(OH)_{0.37(\pm0.05)}(F)_{0.63(\pm0.05)}$. A result obtained consistently in all studied samples is that the terminal site in CJ2 is occupied exclusively by fluorine.

NMR Methods: MQMAS, CP-MQMAS, $^{19}F-^{27}Al$, and $^{19}F-^{31}P$ HETCOR. In this study, several high-resolution solid-state NMR experiments for spin-$^1/_2$ and quadrupolar nuclei were employed.

The standard MAS NMR of ^{19}F has been performed to determine the absolute fluorine content using NaF as an internal reference. The relative fractions of bridging and terminal were determined in the same experiment with ~10% accuracy. These data were used to calculate the relative occupancies of bridged and terminal sites by F and OH.

The technique of multiple quantum magic angle spinning (MQMAS)[12,13] was used to remove the anisotropic line broadening in the NMR spectra of aluminum (Figure 2a). MQMAS was also coupled with the technique of cross polarization, in an experiment referred to as CP-MQMAS,[14,15] to provide high-resolution connectivity and phase

(11) Ubbelhode, A. R. *Molten State of Matter, Melting and Crystal Structure*; Wiley-Interscience: New York, 1978.

(12) Medek, A.; Harwood: J. S.; Frydman, L. *J. Am. Chem. Soc.* **1995**, *117*, 12779.

(13) Frydman, L.; Harwood: J. S. *J. Am. Chem. Soc.* **1995**, *117*, 5367.

(14) Fernandez, C.; Delevoye, L.; Amoureux, J.-P.; Lang, D. L.; Pruski, M. *J. Am. Chem. Soc.* **1997**, *119*, 6858.

(15) Pruski, M.; Lang, D. L.; Fernandez, C.; Amoureux, J.-P. *Solid State NMR* **1997**, *7*, 327.

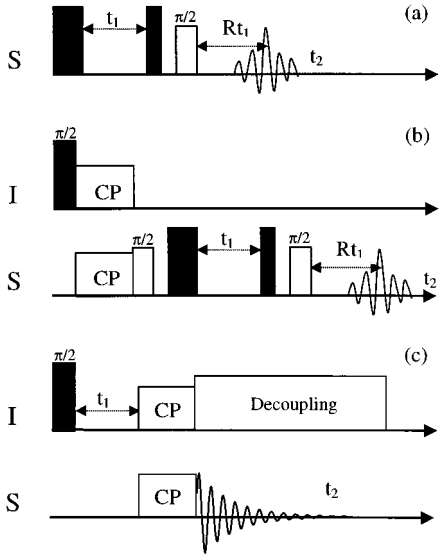

Figure 2. Pulse sequences used in two-dimensional experiments: (a) MQMAS, (b) CPMQMAS, and (c) HETCOR.

separation information (Figure 2b). Finally, heteronuclear correlation[16,17] (HETCOR) experiments between $^{19}F-^{27}Al$ and $^{19}F-^{31}P$ were used to measure the connectivities and resolve the various environments of ^{27}Al, ^{31}P, and ^{19}F in CJ2 (Figure 2c).

The MQMAS experiment is designed to refocus the second-order quadrupolar anisotropy by correlating the evolution of the MQ coherences ($\pm p/2, \mp p/2$) during time t_1 with the observable single-quantum central transition coherence ($-^1/_2, +^1/_2$) during time t_2. Among the various procedures used for obtaining pure absorptive 2D spectra,[12,18−21] we found the *z*-filter method[20] to be the most advantageous. The radio frequency (rf) pulses used to excite the three-quantum coherences ($\pm 3Q$) and to transfer them back to $p = 0$ had an amplitude of ~250 kHz. A selective $\pi/2$ pulse of ~10 kHz rf amplitude was applied after the *z*-filter period of 200 μs. All MQMAS experiments were performed using a sample rotation rate of 20 kHz.

While excitation of MQ coherences via cross polarization can be achieved directly,[22,24] we chose a more approachable coherence transfer scheme ($0 \rightarrow \pm 1 \rightarrow 0 \rightarrow \pm 3 \rightarrow 0 \rightarrow -1$). It is well known that cross polarization of half-integer quadrupolar nuclei is difficult due to the convoluted spin dynamics involved in both the spin locking and the CP processes.[22,24] Work by Sun et al.[22] has shown that efficient spin locking and CP can be achieved using low rf fields and high MAS speed. The CP conditions in our experiments were optimized using an rf field amplitude of ~5 kHz on ^{27}Al, a sample rotation rate of 20 kHz, and a CP contact time of 200 μs.

HETCOR NMR analysis was used to measure the connectivities and resolve the various environments of ^{27}Al, ^{31}P, and ^{19}F in CJ2. In these experiments, the t_1 dimension is inserted, and systematically incremented, just after the initial $\pi/2$ pulse applied to the ^{19}F nuclei (see Figure 2c). Again, the low rf power restrictions for CP between ^{27}Al and ^{19}F were respected with an rf field amplitude of about 8 kHz on ^{27}Al. For the CP between ^{19}F and ^{31}P, higher rf fields of about 20 kHz for ^{31}P and 40 kHz for ^{19}F were used. The HETCOR spectra were acquired at two different magnetic fields, 9.4 and 11.7 T, under MAS at 20 kHz. Contact times for the $^{19}F-^{27}Al$ HETCOR experiments were 150 μs at 9.4 T and 250 μs at 11.7 T. The chemical shifts of ^{19}F, ^{31}P, and ^{27}Al were referenced to $CFCl_3$, H_3PO_4 85%, and aluminum nitrate aqueous solution, respectively.

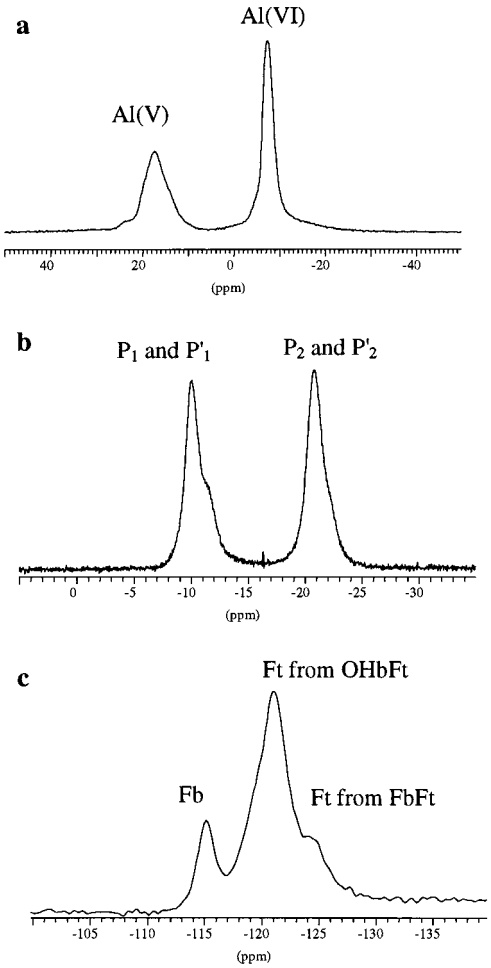

Figure 3. MAS spectra of ^{27}Al (a), ^{31}P (b), and ^{19}F (c) in CJ2(p).

Results and Discussion

1. One-Dimensional ^{27}Al, ^{31}P, and ^{19}F NMR Analysis of CJ2: Quantification of ^{19}F. The first MAS study of $AlPO_4$-CJ2 was reported in our earlier paper.[3] The spectra were obtained for ^{27}Al, ^{31}P, ^{19}F, ^{15}N, and ^{1}H nuclei using a magnetic field of 9.4 T on a powder sample, which had been synthesized over a period of several days. All NMR data were consistent with the results of elemental analysis of the same powder sample and with the X-ray diffraction pattern obtained on a single $AlPO_4$-CJ2 crystal. We have now reexamined the ^{27}Al, ^{31}P, and ^{19}F MAS results using the sample prepared for this study. The MAS spectra of ^{27}Al, ^{31}P, and ^{19}F in CJ2(p) are shown in Figure 3a−c, respectively. In agreement with the previous work, two equally populated aluminum ^{27}Al environments are observed in the spectrum of Figure 3a: hexacoordinated aluminum (Al^{VI}), with the resonance centered at −8 ppm, and pentacoordinated (Al^{V}), with the resonance centered at 17 ppm. As will be later discussed during the analysis of the HETCOR spectra, each of these resonances may include contributions from at least two different Al sites. The two phosphorus sites from our first NMR study are also observed here. They were assigned to the two crystallographically nonequivalent sites P_1 and P_2 that were detected in the XRD analysis. However, a closer examination of the ^{31}P spectra (see Figure 3b) reveals the presence of two

(16) Wang, S. H.; Depaul, S. M.; Bull, L. M. *J. Magn. Reson.* **1997**, *125*, 364.
(17) Steuernagel, S. *Solid State NMR* **1998**, *11*, 197.
(18) Fernandez, C.; Amoureux, J.-P. *Solid State NMR* **1996**, *5*, 315.
(19) Massiot, D.; Touzo, B.; Trumeau, D.; Coutures, J.-P.; Virlet, J.; Florian, P.; Grandinetti, P. J. *Solid State NMR* **1996**, *6*, 73.
(20) Amoureux, J.-P.; Fernandez, C.; Steuernagel, S. *J. Magn. Reson.* **1996**, *A123*, 16.
(21) Brown, S. P.; Heyes, S. J.; Wimperis, S. *J. Magn. Reson.* **1996**, *A119*, 280.
(22) Sun, W.; Stephen, J. T.; Potter, L. D.; Wu, Y. *J. Magn. Reson.* **1995**, *116*, 181.
(23) Vega, A. J. *Solid State NMR* **1992**, *1*, 17.
(24) Vega, A. J. *J. Magn. Reson.* **1992**, *96*, 50.

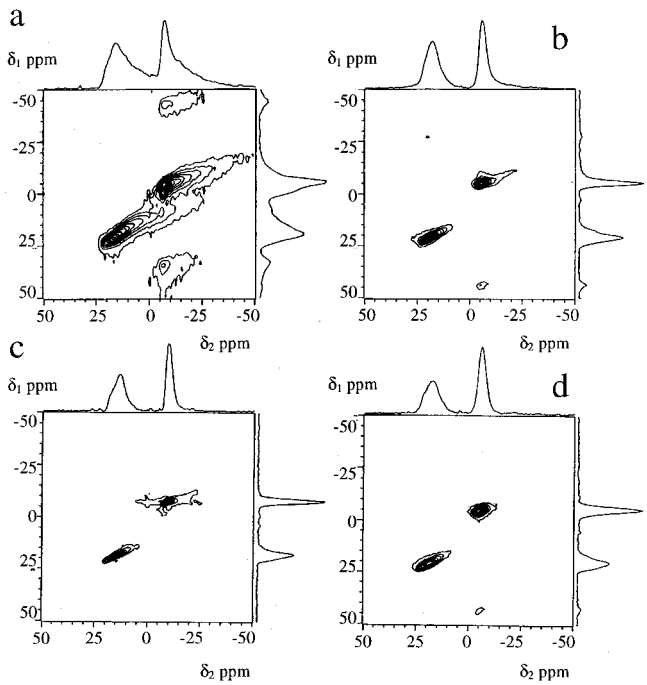

Figure 4. Unsheared 3QMAS and CP-3QMAS spectra: (a) ^{27}Al 3QMAS of CJ2(c), (b) ^{27}Al 3QMAS of CJ2(p), (c) $^{1}H \rightarrow {}^{27}Al$ CP-3QMAS of CJ2(c), and (d) $^{1}H \rightarrow {}^{27}Al$ CP-3QMAS of CJ2(p).

additional shoulders. We denote the main peaks by P_{2a} (−10 ppm) and P_{1a} (−20 ppm) and the additional resonances by P_{2b} (−12 ppm) and P_{1b} (−22 ppm), respectively. We note that $(P_{2a} + P_{2b})/(P_{1a} + P_{1b})$ as well as P_{2a}/P_{1a} and P_{2b}/P_{1b} are all in a 1:1 ratio. The presence of four distinguishable phosphorus environments could not be detected by the XRD method, which did not reveal the distinction between P_{1a}, P_{1b} and P_{2a}, P_{2b}.

Finally, the dominating fluorine resonances, shown in Figure 3c at −115 and −121 ppm (not −116.9 and −122.2 ppm as previously stated[3]), represent fluorine in the bridged and terminal positions, respectively. From the absolute intensity measurements, we found that the fluorine versus OH ratio in the samples used in this study is ∼1.66 (±0.3), which appears to be somewhat lower than the value of 2.0 measured in the sample studied earlier.[3] Furthermore, we determined the ratio of bridged to terminal fluorines to be ∼0.2:1. We note that the terminal peak includes a shoulder on the upfield side located at ∼−124 ppm. In general, four possible configurations can be considered in the SBU structure of Figure 1a: OH_bF_t, F_bF_t, F_bOH_t, and OH_bOH_t. However, a simple analysis of the ^{19}F intensities shows that only $OHbF_t$ and F_bF_t are present in the CJ2 in appreciable amounts with the relative intensities of ∼0.75 and ∼0.25, respectively. Again, the HETCOR spectroscopy results reported herein will provide further insight into the fine structure of the ^{19}F spectra.

2. Two-Dimensional NMR Analysis of Mixed Phases in CJ2. A powder may differ from a single crystal by being a mixture of phases. Often the phase of interest may be mixed with some impurity, or with a phase that has an isotypic structure but not the same composition. In addition, due to the presence of the fractional occupancies at the bridging and terminal sites, the composition of the CJ2 sample is not strictly a "pure" phase. We employed MQMAS and CP-MQMAS to determine the resolution limits of ^{27}Al NMR in CJ2 aluminophosphates and to examine the phase purity of the CJ2(c) and CJ2(p) aluminophosphates described earlier. The ^{27}Al 3QMAS and $^{1}H \rightarrow {}^{27}Al$ CP-3QMAS spectra of both samples are presented in Figure 4.

Two aluminum resonances are resolved in the single-quantum (δ_2) and triple-quantum (δ_1) dimensions of the unsheared 3QMAS spectrum of CJ2(c), each appearing to have a narrower feature superimposed on a broader base (Figure 4a). The lack of significant line narrowing upon application of MQMAS spectroscopy implies that a substantial distribution of isotropic parameters (chemical shifts and quadrupole-induced shifts) must exist in this sample. A striking change in the line widths is readily observed in the δ_2 and δ_1 dimensions of the $^{1}H \rightarrow {}^{27}Al$ CP-3QMAS spectrum of the same sample (Figure 4c). Clearly, the broad lines that dominated the 3QMAS line shape of CJ2(c) are not present in the $^{1}H \rightarrow {}^{27}Al$ CP-3QMAS spectrum, and the narrow features have been singled out. The results become more apparent when the CP-3QMAS spectrum of Figure 4c is compared with a 3QMAS spectrum of the pure phase CJ2(p) sample shown in Figure 4b. The two spectra are almost identical, which shows that CP-3QMAS has successfully isolated the CJ2(p) phase in the mixed phase CJ2(c) sample. Surely, the cross polarization transfer resulted from the dipolar interaction between structural aluminum in CJ2 and the hydrogen atoms in the abundant ammonium template. As expected, the $^{1}H \rightarrow {}^{27}Al$ CP-3QMAS spectrum of the CJ2(p) sample, which is shown in Figure 4d, has exactly the same line shape as those of Figure 4b and c. Thus, the CP-3QMAS method has operated as a phase separation technique for the CJ2(c) sample. We also performed similar $^{19}F \rightarrow {}^{27}Al$ CP-3QMAS experiments. The $^{19}F \rightarrow {}^{27}Al$ CP-3QMAS spectrum of sample CJ2(c) (not shown) resembles that obtained with MQMAS (see Figure 4a), except for the intensity ratio between Al^{VI} and Al^{V}, which was strongly overestimated by the CP process. The broad feature present in this spectrum is consistent with the presence of a highly fluorinated and poorly hydroxylated "AlF_3"-like amorphous phase in CJ2(c). This phase results from its incomplete conversion into CJ2.

We note that the application of CP-MQMAS demonstrated above may be of general interest for templated, microporous materials in which MAS does not provide sufficient resolution.

3. HETCOR NMR Analyses of CJ2(p). We first note that the intensities observed in all HETCOR spectra presented in this work are "filtered" by the cross polarization processes. The spin dynamics involved in these processes is complex and may strongly distort the intensities relative to their corresponding MAS spectra, especially in experiments involving quadrupolar nuclei.[23,24] When necessary, we will revert to the 1D MAS spectra for quantitative information.

3.1. $^{19}F-{}^{27}Al$ HETCOR. Fluorine-to-aluminum connectivities were analyzed using $^{19}F-{}^{27}Al$ HETCOR NMR at two different magnetic fields, 9.4 and 11.7 T. The 2D experiment was repeated several times using various conditions for the spin-locking rf fields, CP contact time, and resonance offsets.

The representative $^{19}F-{}^{27}Al$ HETCOR spectrum consists of four cross-peaks, as shown in Figure 5a. The dominant cross-peak at −121 (^{19}F) and −8 ppm (^{27}Al) can be easily ascribed to the OH_bF_t configuration, as it exhibits a single connectivity between Al^{VI} and F. For the configuration F_bF_t, the F_b fluorine resonates at ∼−115 ppm and exhibits a correlation with both Al^{V} and Al^{VI}. In addition, this configuration should bring about a correlation between F_t and Al^{VI}. Indeed, a third cross-peak is displayed in the HETCOR spectrum as a correlation between the Al^{VI} resonance at −12 ppm and the ^{19}F resonance at −124 ppm. We note that MAS fluorine resonances centered at −115 and −124 ppm have similar intensities, which is another indication that only XF_t configurations exist in CJ2. For the F_bOH_t configuration, if it were present, only a pair of correla-

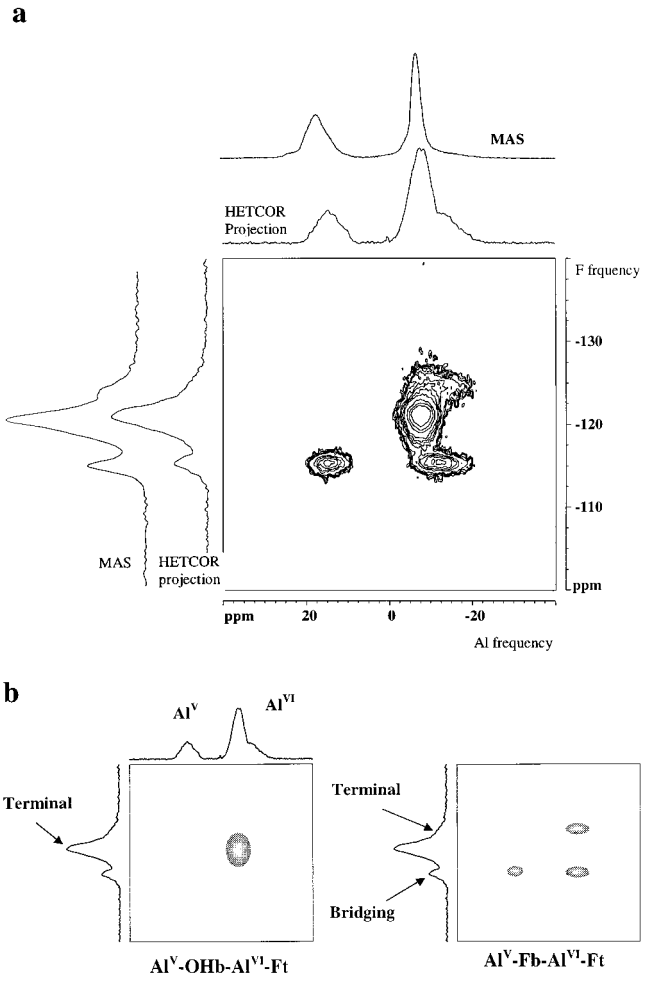

Figure 5. (a) $^{19}F \rightarrow {}^{27}Al$ HETCOR spectrum of $AlPO_4$-CJ2(p). The ^{19}F and ^{27}Al resonances appear along the vertical and horizontal axes, respectively. Experimental conditions: MAS speed, 20 kHz; CP contact time, 250 μs; delay between scans, 4 s; 256 t_1 values with an increment of 20 μs were used with 128 FIDs for each t_1. (b) Assignments of sites and correlations. The corresponding structural unit is given below each panel.

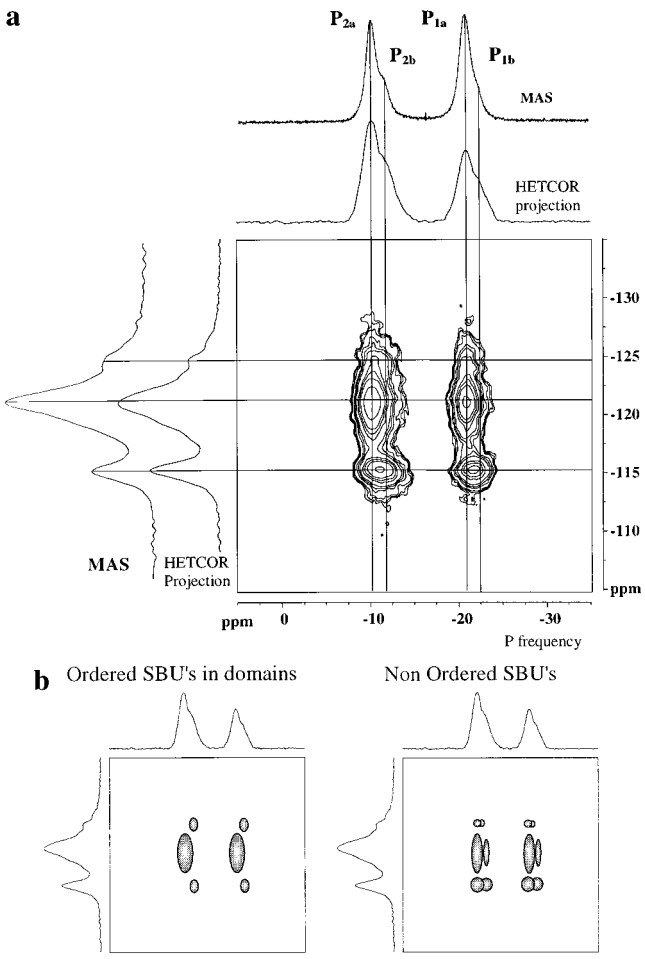

Figure 6. (a) $^{19}F \rightarrow {}^{31}P$ HETCOR spectrum of $AlPO_4$-CJ2(p). The ^{19}F and ^{31}P resonances appear along the vertical and horizontal axes, respectively. Experimental conditions: MAS speed, 20 kHz; CP contact time, 600 μs; delay between scans, 4 s; 192 t_1 values with an increment of 20 μs were used with 56 FIDs for each t_1. (d) Assignments of sites and correlations.

tions between the bridging fluorine at ~−115 ppm and both aluminum environments would be expected. This would lead to a larger intensity of the bridging doublet than is observed in the HETCOR spectrum.

3.2. $^{19}F-{}^{31}P$ HETCOR: Distribution of SBUs in CJ2(p). The correlation spectra between fluorine and phosphorus atoms in CJ2 are shown in Figure 6a. In the phosphorus projection, four ^{31}P resonances, at ca. −10 (P_{2a}), −12 (P_{2b}), −20 (P_{1a}), and −22 ppm (P_{1b}), are clearly visible. The most intense cross-peaks in the $^{19}F-{}^{31}P$ HETCOR spectrum are those between the fluorine at −121 ppm and the phosphorus atoms at −10 and −20 ppm. However, these two cross-peaks are slightly asymmetric in the ^{31}P dimension, suggesting an additional correlation with the phosphorus atoms at −12 and −22 ppm. In addition, correlations appear between the ^{19}F resonance at −115 ppm and all four ^{31}P sites. Finally, the fluorine at −124 ppm is coupled with the phosphorus at −10 and −20 ppm, whereas connectivity with the remaining two phosphorus sites cannot be established with certainty.

The distinction between a structure built of domains containing a single type of SBU or a mixture of different SBUs could not be made on the basis of MAS spectra alone. As will be shown below, such a distinction can be inferred from the analysis of the 2D $^{19}F-{}^{31}P$ HETCOR spectrum of Figure 6a. From the XRD analysis it follows that each phosphorus atom in CJ2 is connected to three separate SBUs.[2] We recall that, within the accuracy of our ^{19}F NMR data, the CJ2 structure contains only OH_bF_t and F_bF_t SBUs in a 3:1 ratio. Therefore, in a hypothetical ordered crystal composed of domains containing the same type of SBUs, each phosphorus site (P_1 or P_2, see Figure 1a) can be found in one of two possible surroundings, connected to either three SBUs of type 1 (OH_bF_t) or three SBUs of type 2 (F_bF_t). The corresponding HETCOR spectrum should exhibit a maximum of six cross-peaks, two representing the OH_bF_t domains and four representing the F_bF_t structures. If the crystal is not organized in domains with a single type of SBU, the number of distinct environments increases. A more complex HETCOR pattern is expected for this structure. Both hypothetical patterns are displayed in Figure 6b. Although resolution of the $^{19}F-{}^{31}P$ HETCOR experiment is limited, the locations and intensities of observed cross-peaks strongly suggest that CJ2 structure does not consist of large domains of SBUs of a single type. Thus, crystallization of CJ2 is likely to occur via nonselective addition of F_bF_t or OH_bF_t SBUs to the growing crystal network.

To make the specific spectral assignments, we first note that, regardless of the structure, the most intense pair of cross-peaks between the ^{19}F resonance at −121 ppm and the ^{31}P resonances at −10 and −20 ppm must correspond to phosphorus surrounded

by three SBUs of type OH_bF_t. The weak correlation that the fluorine line at −121 ppm exhibits with P_{2b} at −12 ppm and P_{1b} at −22 ppm suggests that this terminal fluorine, belonging to OH_bF_t, is also close to an F_bF_t unit. Again, this shows that a significant fraction of F_bF_t units are adjacent to OH_bF_t.

We further note that the cross-peaks at (−115,−12), (−115,−22), (−124,−12,) and (−124,−22) ppm are consistent with the F_bF_t configuration (Figure 6b). Moreover, the P_{2a} and P_{2b} intensities in the HETCOR projection are more intense than those of P_{1a} and P_{1b}, respectively. This is in agreement with the XRD results discussed in the Introduction: each P_2 site is polarized by two F_t and two partially occupied F_b sites, whereas P_1 has only one F_t and one partially occupied F_b neighbor within the 4-Å radius. Furthermore, lines P_{1b} and P_{2b} are enhanced by cross polarization with respect to their MAS values. This is expected if we consider that they correspond to sites in SBU of type 2 with F_bF_t configuration. The interpretation of the $^{19}F-^{31}P$ HETCOR spectrum is schematically depicted in Figure 6b.

Conclusions

Using the NMR techniques MQMAS, CP-MQMAS, and HETCOR on an oxyfluorinated aluminophosphate sample, $AlPO_4$-CJ2, qualitative insight into its structure, purity, and composition was achieved that X-ray diffraction failed to provide. In our study, we found that even a well-defined crystalline powder, giving rise to a "single phase" diffraction pattern, may still contain some amorphous aluminum oxyfluorinated "AlF_3" phase. This phase was effectively "filtered-out" using $^1H \rightarrow {}^{27}Al$ CP-MQMAS, while the well-crystallized fraction of CJ2 was extracted. Similarly, the amorphous "AlF_3" phase was isolated using the technique of $^{19}F \rightarrow {}^{27}Al$ CP-3QMAS. We note that such applications may be of general interest in the analysis of other templated microporous materials.

The ^{19}F intensity measurements and $^{19}F \rightarrow {}^{27}Al$ HETCOR experiments demonstrate that either fluorine or hydroxyl groups can reside in the bridging position. The most abundant type of SBU contains a bridging OH and a terminal fluorine (OH_bF_t). This is the only type of SBU that was seen in the single-crystal study of $GaPO_4$-CJ2.[25] As no hexacoordinated aluminum exists in a prenucleation building unit,[9] the bridging bond is formed when the PNBU enters the crystal. If the lattice host selects only those units that exactly match the place to be filled, then large homogeneous ordered domains would be formed. If the PNBU can adapt its conformation slightly to the available site, or if some flexibility is permitted, then a single crystal made of all possible conformations of the PNBUs can be expected. The latter mechanism of lattice formation appears to be operable during the synthesis of CJ2.

Within a PNBU, changing the aluminum coordination number can modulate the bond lengths around aluminum and, therefore, the interconnecting distances of a PNBU. This can be achieved with or without formation of a bridging species. If there is no bridge formation, the coordination may be increased by addition of nonconnecting groups, e.g., a terminal fluorine or terminal H_2O.

If the coordination change occurs due to the formation of a bridging bond as the PNBU enters the crystal, then unit integration into the network and bridge formation constitute a single chemical step. This may explain why there is no direct relationship between the PNBU and the SBU. It has been a long-standing assumption that the PNBU and the SBU were identical objects. It appears that this assumption is not valid in our case. During their integration into the network, PNBUs may undergo an isomerization that allows them to adapt to the network and transforms them into SBUs.

Acknowledgment. The Centre National de la Recherche Scientifique has funded studies of "Synthesis of oxyfluorinated microporous compounds" under GDR 1164, supporting the Versailles and Strasbourg Groups. The Ministry of French research is acknowledged for funding M.H.'s Ph.D. program. At Ames Laboratory, this research was supported by the U.S. Department of Energy, Office of Basic Energy Sciences, Division of Chemical Sciences, under Contract W-7405-Eng-82. At the University of Lille, the work was sponsored by funding from the Région Nord-Pas de Calais.

JA991295N

(25) Loiseau, T. In *Synthèse et caractérisation par diffractométrie des rayons X et spectroscopie RMN d'une nouvelle famille de microporeux oxyfluorés: les ULM. Un premier pas vers la compréhension des mécanismes réactionnels*; Loiseau, T., Ed.; Université du Maine, 1994.